STEM CELLS AND DEVELOPMENT
Volume 22, Number 3, 2013

DOI: 10.1089/scd.2012.0218

The Generation of Definitive Neural Stem Cells from *PiggyBac* Transposon-Induced Pluripotent Stem Cells Can Be Enhanced by Induction of the NOTCH Signaling Pathway

Ryan P. Salewski,[1,2] Josef Buttigieg,[3] Robert A. Mitchell,[1] Derek van der Kooy,[2,4] Andras Nagy,[2,5] and Michael G. Fehlings[1,2,6,7]

Cell-based therapies using neural stem cells (NSCs) have shown positive outcomes in various models of neurological injury and disease. Induced pluripotent stem cells (iPSCs) address many problems associated with NSCs from various sources, including the immune response and cell availability. However, due to inherent differences between embryonic stem cells (ESCs) and iPSCs, detailed characterization of the iPS-derived NSCs will be required before translational experiments can be performed. Murine piggyBac transposon iPSCs were clonally expanded in floating sphere colonies to generate primitive NSCs initially with serum-free media (SFM) containing the leukemia inhibitory factor and followed by SFM with the fibroblast growth factor-2 (FGF2) to form colonies of definitive NSCs (dNSCs). Primitive and definitive clonally derived neurospheres were successfully generated using the default conditions from iPSCs and ESCs. However, the iPSC-dNSCs expressed significantly higher levels of pluripotency and nonectoderm lineage genes compared to equivalent ESC-dNSCs. The addition of the bone morphogenetic proteins antagonist, Noggin, to the media significantly increased primary neurosphere generation from the iPSC lines, but did not affect the dNSC sphere colonies generated. The induction of the NOTCH pathway by the Delta-like ligand 4 (DLL4) improved the generation and quality of dNSCs, as demonstrated by a reduction in pluripotency and nonectodermal markers, while maintaining NSC-specific gene expression. The iPS-dNSCs (+DLL4) showed functional neural differentiation by immuncytochemical staining and electrophysiology. This study suggests the intrinsic differences between ESCs and iPSCs in their ability to acquire a dNSC fate that can be overcome by inducing the NOTCH pathway.

Introduction

Neurotrauma, including brain and spinal cord injury (SCI), is a significant cause of mortality and neurological morbidity. Despite advances in medical and surgical care, there are limited treatments for many neuropathological indications, specifically in conditions resulting from loss of cells or cellular functions, such as SCI or Parkinson's. The replacement of neural cells lost by injury, autoimmune, or other pathological mechanisms has tremendous promise to treat these neurological insults [1]. Embryonic stem cell (ESC)-derived and adult-derived neural stem cells (NSCs) have been shown to be an effective treatment for a number of neurological insults, including SCI [2–4], Parkinson's [5], multiple sclerosis [6], and spinal muscular atrophy [7].

Despite positive preclinical results for these cells, concerns for each cell source exist. For example, NSCs from adult tissue have limited availability for clinical situations, while ESCs often lack a clear NSC stage before clinical use, as well as posing ethical challenges. The development of induced pluripotent stem cells (iPSCs) could revolutionize the field of regenerative medicine by addressing many of these issues [8,9]. Although a recent study showed that iPSCs may still evoke an immune response following syngenic transplants, these cells are still likely to be superior to heterologous transplantation [10]. This finding, along with their ready

[1]Division of Genetics and Development, Toronto Western Research Institute, Toronto, Canada.
[2]Institute of Medical Science, University of Toronto, Toronto, Canada.
[3]Department of Biology, University of Regina, Regina, Canada.
[4]Department of Molecular Genetics, University of Toronto, Toronto, Canada.
[5]Samuel Lunenfled Research Institute, Mount Sinai Hospital, Toronto, Canada.
[6]Spinal Program, University Health Network, Toronto Western Hospital, Toronto, Canada.
[7]Division of Neurosurgery, University of Toronto, Toronto, Canada.

availability and the lack of requirement for embryonic tissues, makes iPSCs an attractive source for cell-based therapies. Initially, iPSC technology was criticized due to the requirement for viral integration of transgenes into the cell genome. There are now multiple strategies to generate iPSCs without viral genomic integration with varying efficiency [11–13]. Specifically, the piggyBac (PB) transposon method, used to generate the iPSCs in this study, allows for the induction of pluripotency using the standard reprogramming factors (*Oct4, Sox2, Klf4*, and *c-myc*) delivered in a single vector. Once the pluripotent state is stable, the transgene cassette can be seamlessly excised [11,14]. Even though nonmutagenic and nonviral methods have been developed to generate iPSCs, concerns, such as epigenetic differences [9], still exist regarding whether the reprogrammed cells are equivalent to their ESC counterparts [15].

Simply transplanting pluripotent cells into an organism has tremendous potential for teratoma formation, therefore pluripotent cells will need to be directed to restricted neural precursors before use in regenerative medicine. An effective method to generate clonally derived neurospheres from murine pluripotent cells is the default pathway of neuralization [16,17]. At low cell density, in the absence of external cues, pluripotent cells acquire a neural identity. A small percentage of pluripotent cells cultured under serum-free and low cell density conditions proliferate in the presence of leukemia inhibitory factor (LIF) to form floating sphere colonies of primitive NSCs (pNSCs) that express the neuroepithelial markers, nestin and Sox1 [17]. Moreover, a small proportion of cells derived from primitive neurospheres can generate neurospheres made up of definitive NSCs (dNSCs) when subcloned, independent of LIF, in the presence of fibroblast growth factor-2 (FGF2) [16,18,19]. The pNSCs from a pluripotent source have been shown to be similar to NSCs derived from E5.5–7.5 embryos [20], while dNSCs are akin to those isolated at E8.5 and after from the embryo [18]. This pathway can be reinforced using specific inhibition of bone morphogenetic proteins (BMP), a member of the transforming growth factor-β family that promotes a non-neural fate acquisition. Noggin, a BMP-specific inhibitor, has been demonstrated to significantly increase the number of primary neurospheres obtained from ESCs when using the default pathway [16]. Also, the NOTCH pathway plays a key role in neurodevelopment and persists in the adult nervous system to regulate NSCs [21,22]. Disruptions in NOTCH have been associated with a reduction in NSC number [23,24], while its activation stimulates NSC proliferation in vivo [25]. Delta-like ligand (DLL) and Jagged are the principal ligands for the NOTCH receptor in the NSC niche of the subventricular zone (SVZ), which regulate the proliferation and self-renewal of NSCs [26]. Canonical NOTCH signaling involves a membrane ligand binding with the NOTCH receptor. The NOTCH intracellular domain (NICD) is cleaved by γ-sereatase. NICD translocates to the nucleus, coactivators are recruited, and target genes, such as Hair and enhancers of split (Hes) genes, are transcribed [27].

Ineffective generation of dNSCs or retention of pNSC characteristics could limit the use of iPSC technology in cell-based therapy or in disease modeling. In this study, we demonstrate that intrinsic differences exist between our murine ESCs and PB-iPSC lines in their ability to generate dNSCs. The overarching goal of this work is to exogenously manipulate the signaling pathways to consistently generate iPS-dNSCs that behave similarly to ES-dNSCs and adult tissue-derived NSCs. We hypothesize that the activation of the NOTCH pathway during the generation and maintenance of iPS-dNSCs will significantly improve their neuralization, thereby increasing their clinical relevance and translational potential.

Materials and Methods

ES/iPS expansion culture

R1 and G4 murine ES cells as well as C5, C5-4A, and B1-1G murine iPS cells were used in all experiments. All cell lines express the green fluorescent protein (GFP). Additional information regarding the cell lines is supplied in Supplementary Table S1 (Supplementary Data are available online at www.liebertpub.com/scd).

The ES/iPS cells were cultured using a standard serum and feeder layer conditions [28]. In brief, the ES/iPS cells were plated on NUNC-coated dishes on a mitomycin C inactivated mouse embryonic fibroblast (MEF) feeder layer in media containing Dulbecco's modified Eagle's medium, ESC qualified fetal bovine serum (FBS), L-glutamine, penicillin/streptomycin, nonessential amino acids, β-mercaptoethanol + LIF (1,000 U/mL; Millipore). For passage, the confluent cells were incubated with 0.05% trypsin–ethylenediaminetetra acetic acid for disassociation and plated at a 1:5 ratio.

Generation of primitive and definitive neurospheres

The generation of primitive and definitive neurospheres followed the protocol previously described [16,28]. ESC/iPSCs were disassociated using TrypLE Select (Invitrogen) and spun at 1,500 rpm for 5 min. Cells were resuspended in ES/iPS media and plated on NUNC-coated dishes so that MEFs were able to attach. The supernatant was collected and spun down and rinsed twice with serum-free media (SFM) [29]. For primary pNSC, ES/iPSCs were seeded in low-attachment flasks at cell density of 10 cell/μL in SFM containing LIF (1,000 U/mL). Primary primitive neurospheres were present after 7 days, upon which single neurospheres could be dissociated using TrypLE Select and in SFM media + LIF (Millipore), FGF2 (10 mg/100 mL; Sigma), and heparin (2 mg/100 mL; Sigma) to yield secondary primitive neurospheres. These cells were repassaged at 10 cells/μL in the SFM + LIF, FGF2, and heparin to yield tertiary primitive neurospheres and so on. To generate dNSCs following pNSC passage 3, the cells were seeded at 10 cells/μL in SFM without LIF, containing only FGF2 and heparin. B27 supplement (Gibco) was added to increase cell survival. The dNSCs can be continually passaged in the SFM + FGF, heparin, and B27. The cell culture process is outlined in Supplementary Fig. S1.

Noggin treatment

During the initial transition from the pluripotent conditions to the primary pNSC conditions, Noggin (250 ng/mL, R&D system) was used in addition to the culture conditions outlined above (Fig. 2). Noggin treatment groups included single passage exposure solely during the initial neuralization as well as continual exposure during the 3 pNSC passages. We compared these groups with the non-

Noggin-treated pNSCs. Also, iPSCs that received pretreatment with Noggin during the final day of iPSC expansion conditions were examined for neurosphere generation during initial induction of primary pNSCs.

NOTCH pathway induction and inhibition

DLL4 is an agonist of the Notch pathway. Recombinant mouse DLL4 (R&D systems; 500 ng/mL) was added to the definitive cell culture condition and maintained continuously during dNSC expansion. N-[N-(3,5-Difluorophenacetyl)-L-alanyl]-S-phenylglycine t-butyl ester (DAPT; Sigma; 1 μM) a γ-secretase inhibitor that blocks NOTCH cleavage was also added to definitive cell culture condition as a NOTCH inhibition control.

Neurosphere assay

The pluripotent iPSCs were seeded at 10 cells/μL with SFM + LIF in the center 24 wells of a 48-well plate. About 3,000 cells in 300 μL of media were plated in each well. Seven days following induction of neuralization conditions, the wells were analyzed for floating spheres. Counts were made using an inverted microscope with a calibration grid. Definitive neurospheres were quantified in the same manner.

Real time-polymerase chain reaction

The mRNA was isolated from pNSCs and dNSCs using the RNeasy Micro Kit (Qiagen). To evaluate the concentration and purity of mRNA, the samples were analyzed using a Nanodrop. About 150–500 μg mRNA was used to synthesize cDNA using Superscript III with Oligo-DT (Invitrogen) according to instructions. Real-time-polymerase chain reaction (RT-PCR) was performed using TAQman designed primers with FAST TAQman master mix under described thermocycling (50°C–2 min, 95°C–20 s, 40 cycles of 95°C–1 s, 60°C–20 s) on a 7900HT Real-time PCR system. Samples (5 ng of cDNA used per reaction well) were run in triplicate along with a negative (no template) control. All values were normalized to the endogenous control (GAPDH) that was consistent among all samples. Results were compared to their pluripotent cell sources grown in feeder-free conditions using Matrigel-coated plates with MEF-conditioned media. Gene expression levels were compared using the $2^{-\Delta\Delta CT}$ method [30]. TAQman sequences are proprietary and can be found at www.appliedbiosystems.com (Supplementary Table S2).

Cryopreservation of neurospheres

Neurospheres were collected 7 days following passage and were fixed with 4% paraformaldehyde (PFA) followed by cryopreservation in 30% sucrose solution. The neurospheres were embedded in the OCT medium, frozen on dry ice, and sectioned at 20 μm using a cryostat. The slides were stored at −80°C until analysis using immunocytochemistry.

Differentiation assay

Passage 4 dNSCs from iPSC sources were dissociated to a single-cell suspension and plated in 8-well chamberslides (BD Bioscience) coated with growth factor-reduced Matrigel (BD Biosystems). The cells were plated at a density of 25 cell/μL in SFM without growth factors and containing 1% FBS to induce differentiation [3]. Following 1 week of differentiation conditions, the cells were fixed with 4% PFA for immunocytochemistry. For electrophysiological analysis, the iPS-dNSC(+DLL4) cells were plated in the same conditions as above on glass coverslips coated with Matrigel.

Immunocytochemistry

Samples from both the differentiation assay and the cyropreserved neurospheres were analyzed using standard immunocytochemical procedures. In brief, the 4% PFA fixed GFP expressing iPS-dNSCs were incubated with phosphate-buffered saline containing 1% bovine serum albumin, 5% normal goat serum, 5% nonfat milk powder, and 0.25% Triton X-100 for 1 h to block nonspecific binding. The slides were incubated overnight at 4°C with a primary antibody (Supplementary Table S3) diluted in the same blocking solution. The slides were incubated for 1 h with an appropriate secondary antibody (Invitrogen). Last, slides were mounted with the Vectashield mounting medium with 4′,6-diamidino-2-phenylindole (DAPI) (Vector Labs) for nuclear counterstaining.

Differentiated cell counting

Three sets of differentiated dNSCs from distinct iPSC sources were labeled for markers of differentiation. For each immunocytochemistry experiment, 8 separate wells per primary antibody were stained and 4 random nonoverlapping images were taken using a confocal microscope, within each stained well. DAPI was used as a nuclear counterstain to evaluate total cell numbers. The proportion of undefined cells was calculated by subtracting the percentage of cells positive for Nestin, Olig2, GFAP, and βIII tubulin from the total cell count. The cell counting was performed from confocal images using ImageJ cell counting software (ImageJ, U.S. National Institutes of Health, http://rsb.info.nih.gov/ij/, 1997–2007).

Electrophysiology

Nystatin perforated patch recordings were made using an Axon multiclamp 700B and signals were filtered with a low-pass 5-kHz filter, digitized (Digidata 1300 series) at a 32-kHz rate, and stored and analyzed on a computer using Clampfit 9 software (Molecular Devices). At the beginning of all experiments ~90% of the series resistance was compensated, and junction potentials were cancelled. In voltage-clamp experiments, cells were held at −60 mV and step depolarized to the indicated test potential (between −100 and +80 mV in 10 mV increments) for 100 ms at a frequency of 0.1 Hz. Patch pipettes were made from borosilicate glass (World Precision Instruments) using a vertical puller (PP 83; Narishige), with a resistance of 6–10 MΩ. The pipette solution contained (mM): K gluconate, 110; KCl, 25; NaCl, 5; $CaCl_2$, 2; HEPES, 10; at pH 7.2, and nystatin (300–450 μg/mL). The bath solution contained: $NaHCO_3$, 24; NaCl, 111; KCl, 5; $CaCl_2$, 2; $MgCl_2$, 2; glucose, 10; and was bubbled with 5% CO_2/95% O_2. Bath temperature was maintained at 37°C. To facilitate later identification of recorded cells in cell cultures, the pipette solution also contained 5% (w/v) aqueous solution of Lucifer Yellow (Sigma). In cell cultures, after visual identification, a glial cell was approached with a patch pipette using

a Burleigh PCS 5000 series micromanipulator. The pipette was pressurized (10 mmHg) to help prevent contamination of the tip. After approaching the cell membrane surface, the pressure was released and a gigaseal was formed. After electrophysiological recordings, the cell type was confirmed using immunocytochemistry as described above.

Statistical analysis

A Student's unpaired *t*-test or one-way analysis of variance was done with the Bonferroni correction applied for pairwise comparisons of subgroups. Results were considered to be statistically significant if $P < 0.05$. Statistical analysis was performed using Microsoft Excel.

Results

ESCs and iPSCs respond differently to neuralization conditions

ESC and iPSC populations were expanded using traditional ES culture conditions and directed through the default pathway using serum-free conditions to primitive (LIF-dependent) and definitive (FGF-dependent) NSCs. Phase-contrast microscopy during each stage of neuralization elucidated the qualitative differences between the ESC and iPSC sources for NSCs. There were no qualitative differences between the ESCs and iPSCs during pluripotent expansion culture (Fig. 1A, left) or during the generation of pNSCs

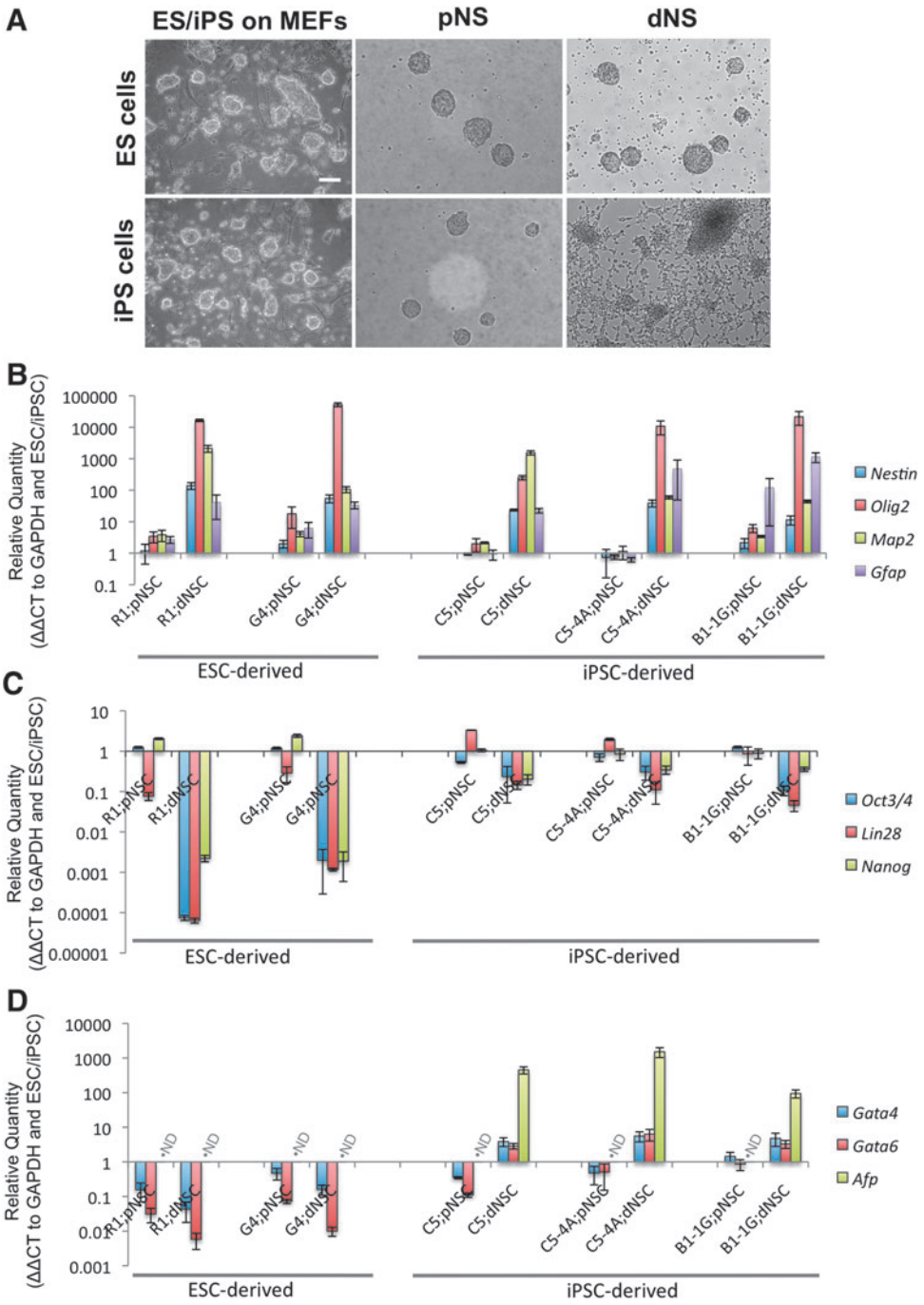

FIG. 1. ESCs and iPSCs have variable neural propensity using the default pathway conditions. **(A)** Phase-contrast microscopy images of ESCs (*upper*, *left*) and iPSCs (*lower*, *left*) on a feeder layer, LIF-dependent primitive neurospheres (pNS; *center*), FGF-dependent definitive neurospheres (dNS; *right*). The ES-derived dNS (*upper*, *right*) show a free-floating phenotype, while the iPS-derived dNS (*lower*, *right*) show a considerable amount of adhesion and differentiation. **(B–D)** iPS-dNSCs show an increase in neural gene transcription. However, iPS-dNSCs retained pluripotency and endodermal gene expression compared to ES-dNSC controls. **(B)** Neural-specific markers are significantly increased in the ESC- and iPSC-derived dNSCs. **(C)** Pluripotency genes are altered as iPSCs follow the default pathway, however, to a lesser extent than the ESCs. **(D)** Endodermal lineage gene markers remain present in the iPS-dNSCs. ND denotes not detected; mean ± SEM; $n = 3$; scale represents 75 μm (R1 and G4 ES lines. C5, C5-4A, and B1-1G iPSC lines). ESCs, embryonic stem cells; iPSCs, induced pluripotent stem cells; LIF, leukemia inhibitory factor; FGF, fibroblast growth factor; NSCs, neural stem cells; dNSCs, definitive NSCs; ES, embryonic stem; ESC, embryonic stem cells; SEM, standard error of the mean.

(Fig. 1A, center). However, upon transition from the primitive to dNSC condition, the dNSCs from the iPS cell population showed adhesion and differentiation during neurosphere generation condition, where ESC-dNSC formed floating spheres (Fig. 1A, right).

To quantify the difference in the neuralization effectiveness and efficiency of the ESC- and iPSC-derived NSCs, a number of key neural stem/progenitor cell-specific (*Nestin*, *Olig2*, *Map2*, and *GFAP*), pluripotency (*Oct3/4*, *Lin28*, and *Nanog*) and nonectodermal (*Gata4*, *Gata6*, and *Afp*) markers were examined using RT-PCR. Also, 2 ESC and 3 iPSC lines were used to ensure that the differences were not cell line-specific variations. The gene marker profile of pNSCs was similar across both ESCs and iPSCs with some variability within the first logimetric unit (Fig. 1B–D). The neural markers examined displayed similar profiles in the dNSCs from ESC and iPSC sources (Fig. 1B). The ES-dNSCs showed an exponentially greater decrease in pluripotency gene mRNA compared to the iPS-dNSCs (Fig. 1C). Finally, there was an increase in endoderm lineage-specific gene markers in the iPS-dNSCs, where the same markers were deceased or at such low levels that they could not be detected by the assay in the ES-dNSCs (Fig. 1D).

BMP antagonism increases neurosphere generation

The default pathway of neuralization relies on the absence of cues directing pluripotent cells to non-neural lineages. BMPs play a key role in directing cells to endoderm lineage. Noggin, a potent BMP antagonist, was added to cell culture conditions. There was a significant increase in the number of primary neurospheres generated from C5-4A iPSCs with Noggin in the media (Fig. 2A; $P < 0.001$). Also, pretreatment of pluripotent cells with Noggin in the expansion media did not affect primary neurosphere generation. Even with Noggin pretreatment, there was increased neurosphere generation with Noggin (Fig. 2A; $P < 0.001$). RT-PCR was used to evaluate the neural (Fig. 2B), pluripotency (Fig. 2C), and endodermal (Fig. 2D) gene profile of third passage iPS-pNSCs that received continuous Noggin, an initial single Noggin, or no Noggin treatment. Noggin treatment had no effect on the mRNA profile of the iPS-pNSCs. Furthermore, there was no change in the mRNA profile of the subsequent iPS-dNSCs generated from the Noggin-treated cells (data not shown). These data suggest that the variability in neuralization of the iPSCs is unlikely to be a function of the initial neuralization cues of the default pathway.

NOTCH pathway agonism improves the neuralization of the iPSC-derived dNSCs

The NOTCH pathway was induced during the transition from primitive to definitive conditions by the addition of recombinant mouse DLL4 to the definitive media and maintaining it during dNSC passage. The effect of NOTCH signaling on the number of definitive neurospheres generated was evaluated (Fig. 3A). The addition of DLL4 to the definitive media resulted in a significant increase in definitive neurospheres compared to definitive media alone by the third passage. There was a significant decrease in neurosphere number when NOTCH signaling was inhibited using DAPT. The DAPT-treated cells failed to yield neurospheres by the third passage. iPS-dNSCs(+DLL4) showed enhanced definitive neurosphere generation and reduced adherence compared to nontreated cells demonstrated using phase-contrast microscopy of passage 4 definitive neurospheres (Fig. 3B). The iPS-dNSCs showed considerable evidence of

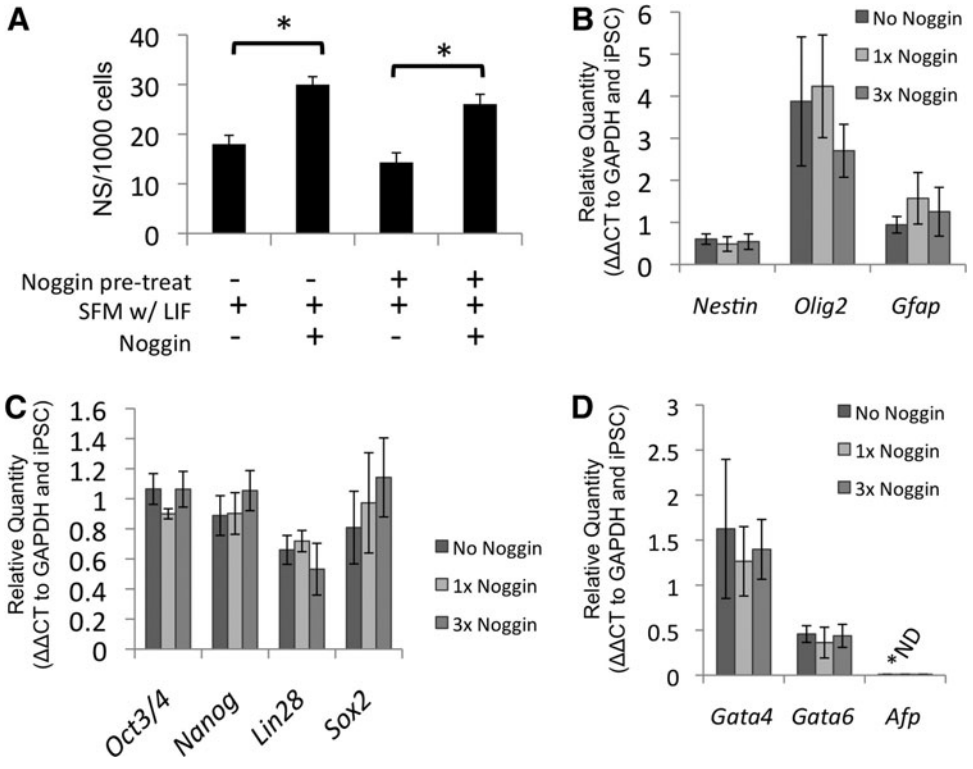

FIG. 2. Noggin increases primary iPSC-derived neurosphere generation. **(A)** The number of primary primitive neurospheres generated following 7 days of culture in SFM + LIF with and without Noggin was evaluated from iPSCs grown on MEFs with and without Noggin pretreatment. The presence of Noggin in the SFM + LIF evoked a significant increase in neurosphere number regardless of Noggin pretreatment. Selected neural **(B)**, pluripotency **(C)**, and endodermal **(D)** gene markers were examined in the passage 3 pNSCs cultured without Noggin (No Noggin), with a single passage with Noggin (1×Noggin), or with continuous Noggin treatment (3×Noggin). No significant differences were detected. C5-4A iPSC line. ND denotes not detected; mean ± SEM; $n = 3$, $^*P < 0.05$. SFM, serum-free media; pNSC, primitive NSC.

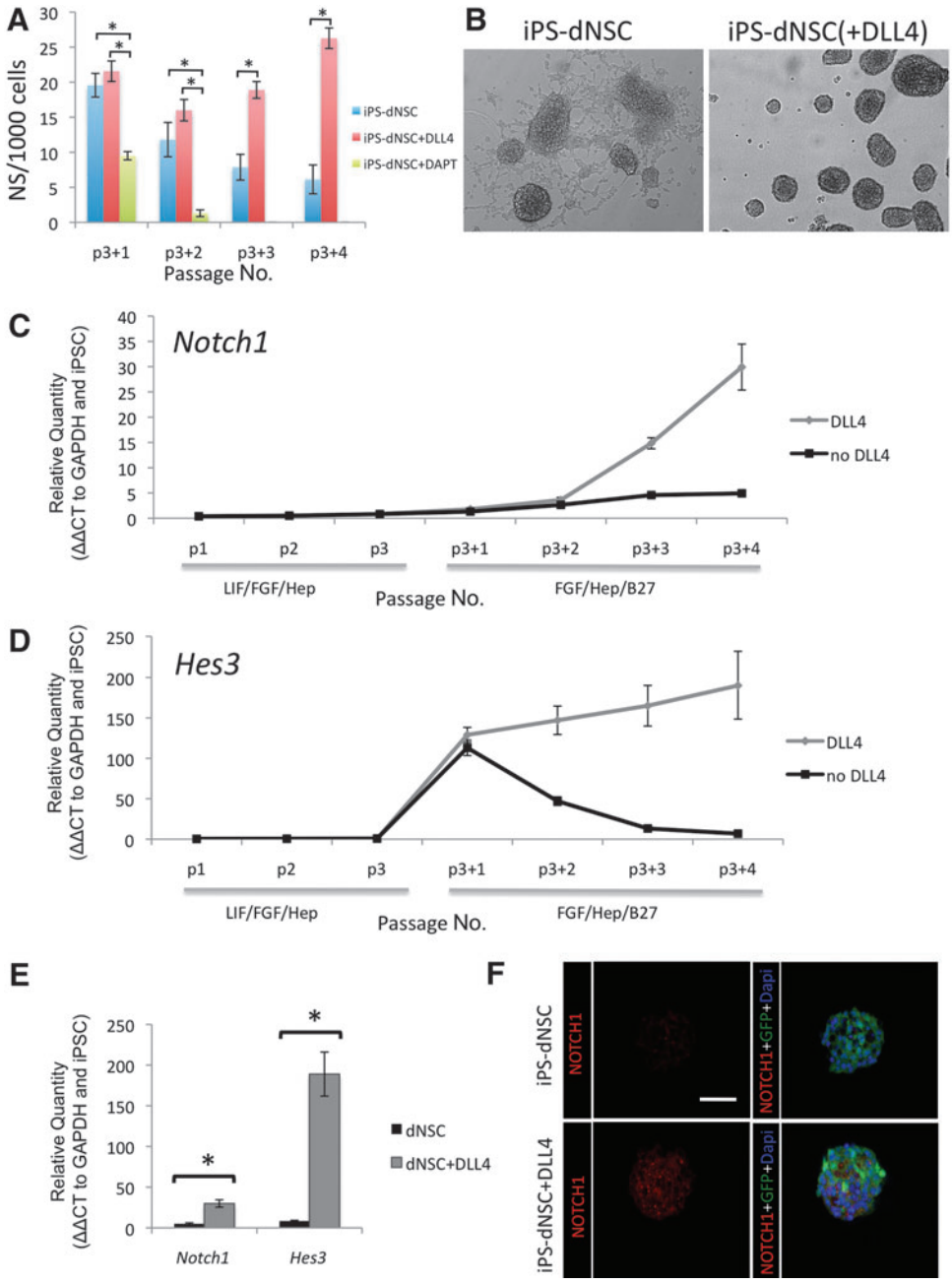

FIG. 3. The addition of DLL4 significantly increased NOTCH pathway genes in iPS-dNSCs. **(A)** The number of neurospheres per 1,000 cells in definitive media conditions alone, with DLL4 or with DAPT was evaluated. The addition of the NOTCH pathway inhibitor DAPT resulted in significantly fewer neurospheres and failure to form spheres beyond the second passage. Significantly more definitive neurospheres were formed in the presence of DLL4. **(B)** Phase-contrast microscopy images of passage 4 iPS-derived definitive neurospheres (*left*) and iPS-derived definitive neurospheres with DLL4 (*right*). The iPS-derived definitive neurospheres show a considerable amount of adhesion and differentiation compared to iPS-derived definitive neurospheres cultured with DLL4. **[(C, E)** *left*] Notch1 gene expression is significantly increased in iPS-dNSCs by the fourth passage in definitive conditions with DLL4 in the media compared to the definitive media alone. **[(D, E)** *right*] HES3, a downstream mediator of NOTCH, increases in iPS-dNSCs with a single passage in definitive media regardless of DLL4 treatment, however, without exogenous DLL4 treatment, HES3 expression returns to baseline levels by passage 4. **(F)** Immunolabeling for receptor Notch1 on cryopreserved definitive neurospheres with and without DLL4 agonism. C5-4A iPSC line. mean ± SEM; $n = 4–5$, $^*P < 0.05$ scale bar represents 75 μm. DLL4, Delta-like ligand 4; DAPT, N-[N-(3,5-Difluorophenacetyl)-L-alanyl]-S-phenylglycine t-butyl ester.

adhesion and differentiation morphology, while the iPS-dNSCs(+DLL4) maintained a free-floating sphere phenotype. The frequency and appearance of iPS-dNSC(+DLL4) was similar to that observed with ES-dNSC or adult neural precursor cell colonies (Data not shown). The effect of DLL4 was evaluated by quantifying the gene expression of the NOTCH receptor, *Notch1*, as well as its downstream targets, *Hes1 and Hes3*. *Notch1* gene transcription increased over the 4 passages in definitive media with DLL4 compared to cells passaged in parallel without DLL4 (Fig. 3C, E; $P = 0.002$). The

downstream effector of the NOTCH receptor activation, *Hes3*, also showed an increase in mRNA transcription during the definitive media passages (Fig. 3D, E; $P<0.001$). *Hes3* expression increased expression in the definitive conditions in both DLL4 and nontreated cultures during the first passage. However, *Hes3* expression was maintained in the iPS-dNSC(+DLL4), while the nontreated cells lost *Hes3* expression during the 4 passages (Fig. 3D, E). The loss of *Hes3* expression correlated with the decreased quantity of neurospheres per passage and eventual inability to passage cells. *Hes1* gene expression was not altered by DLL4 (Supplementary Fig. S2). The increase in *Notch1* in dNSC(+DLL4) was supported with data from immunocytochemistry for Notch1 receptor on cyropreserved, sectioned neurospheres (Fig. 3F). Both NOTCH1 and HES3 are upregulated in ESC-derived dNSCs (Supplementary Fig. S3). These results support the hypothesis that insufficient NOTCH signaling may be involved in the variable neuralization of the iPSCs.

Furthermore, a panel of key neural, pluripotency, and nonectoderm genes were examined in 2 distinct factor-removed iPSC lines (C5-4A, B1-1G) at the first and fourth definitive passage, ± DLL4 treatment. The initial passage in definitive media resulted in an mRNA profile that was intermediate between primitive and definitive characteristics. Furthermore, the addition of DLL4 did not affect this profile (Supplementary Fig. S4). For fourth passage dNSCs, the neural marker panel showed significant increases in the neural specific markers, *Nestin* (C5-4A, $P=0.021$; B1-1G, $P=0.006$), *Olig2* (C5-4A, $P=0.020$; B1-1G, $P=0.046$), and *Mash1* (C5-4A, $P=0.028$; B1-1G, $P=0.045$) with DLL4 treatment compared to controls (Fig. 4A). The pluripotency panel showed significant decreases in *Oct4* (C5-4A, $P=0.014$; B1-1G, $P=0.018$), *Lin28* (C5-4A, $P=0.018$; B1-1G, $P=0.005$), and *Nanog* (C5-4A, $P=0.041$; B1-1G, $P=0.009$) with DLL4 treatment compared to controls, while *Sox2*, a pluripotency marker maintained in NSCs, exhibited similar expression levels (Fig. 4B). Last, the nonectoderm gene panel

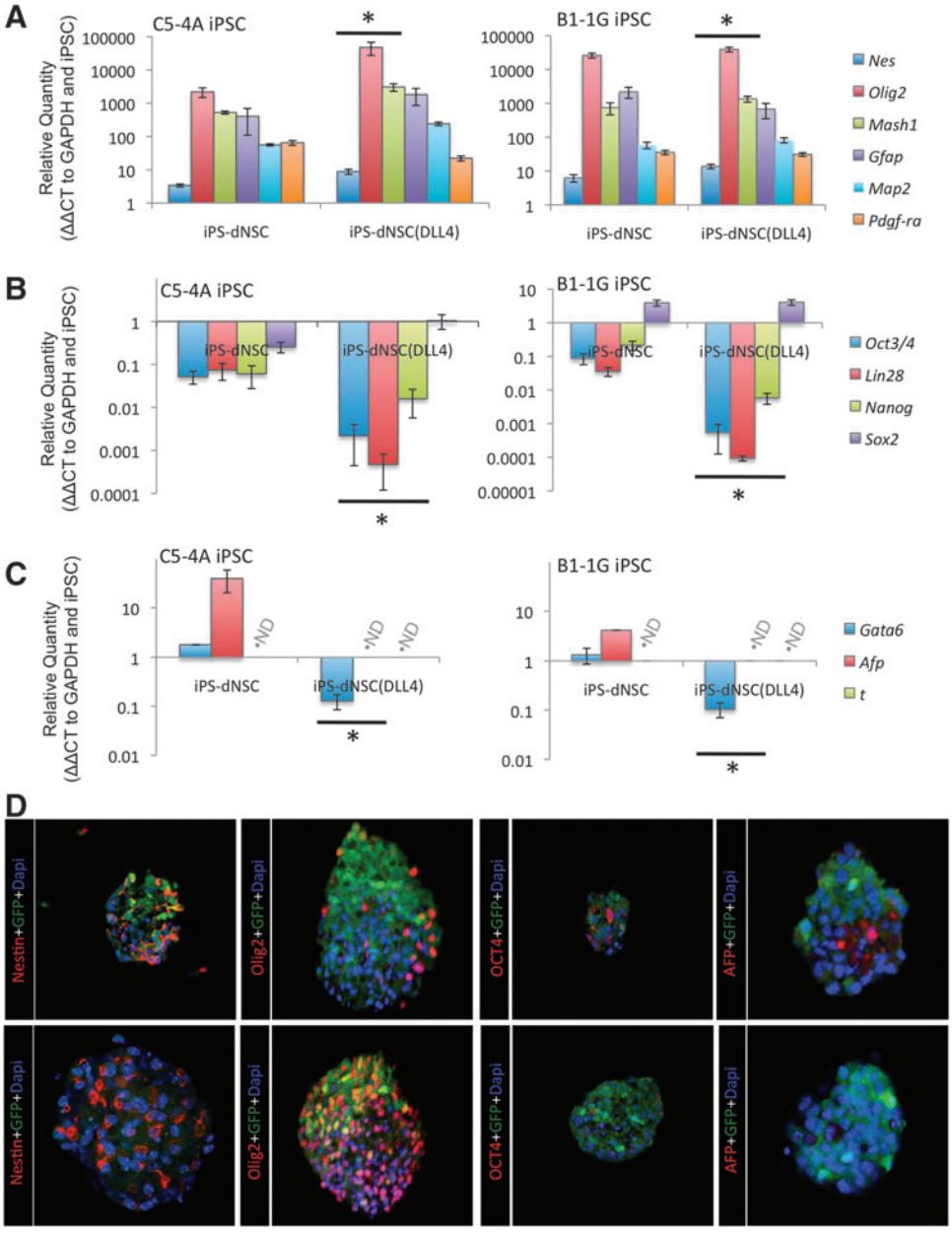

FIG. 4. iPS-dNSCs cultured in definitive media conditions with DLL4 exhibit a more neural-specific gene expression profile compared to iPS-dNSCs cultured in definitive media alone. Selected neural **(A)**, pluripotency **(B)**, and nonectoderm **(C)** gene markers were examined in the iPS-dNSCs (C5-4A; *left* and B1-1G; *right*) cultured with and without DLL4. The addition of DLL4 significantly reduced residual pluripotency and endodermal markers, while maintaining the neural character of the cells. Cyropreserved passage 4 definitive neurospheres for C5-4A cell line cultured in definitive media without DLL4 (*upper panels*) or with continuous DLL4 treatment (*lower panels*) were sectioned and stained for NSC markers [**(A)** nestin, **(B)** Olig2], a pluripotency marker [**(C)** Oct4], and a pan-endoderm [**(D)** Afp] (C5-4A iPSC line). ND denotes not detected; mean ± SEM; $n=4$–5, $^*P<0.05$ compared to iPS-dNSC grown without DLL4; scale bar represents 100 μm.

showed an increase in the endoderm gene markers, *Gata6* and *Afp*, in the non-DLL4-treated cells, while addition of DLL4 to culture condition resulted in a significant decrease in *Gata6* expression (C5-4A, $P<0.001$; B1-1G, $P=0.036$) and no detectable *Afp* mRNA (C5-4A, $P=0.005$; B1-1G, $P<0.001$; Fig. 4C). The mesoderm gene marker, *Brachyury*(*T*), was not detected in either cell group (Fig. 4C). Cyropreserved neurospheres from fourth passage iPS-dNSCs (C5-4A iPSC line) were examined using immunocytochemistry to support key findings from RT-PCR experiments. Immune labeling for *Nestin*, *Olig2*, *Oct4*, and *Afp* in the NOTCH-agonized cell group reinforced the finding of improved neuralization with the iPS-dNSC(+DLL4) treatment (Fig. 4D).

DLL4-treated iPS-dNSCs differentiate toward neural cells more efficiently than nontreated cells

Fourth passage iPS-dNSC neurospheres were dissociated to single-cell suspension and plated on chamberslides coated with Matrigel at a density of 25 cells/μL in media without growth factors and containing 1% FBS to induce differentiation. Cells were examined 1 week following exposure to differentiation conditions. Representative immunofluorescence images of neural differentiation markers (GFAP, astrocytes; Olig2, pan-oligopercursor/oligodentrocyte; PDGFra, oligodendrocytes; βIII tubulin, neurons; Nestin, neural precursor cells) are shown in Fig. 5A. The greatest difference observed was in the GFAP and Nestin labeling, where extensive GFAP+ and limited Nestin+ cells were seen in iPS-dNSCs(+DLL4) compared to iPS-dNSCs, which yielded mostly Nestin+ cells. The number of immunofluorescent-positive cells was counted in nonoverlapping microscope fields for each of the neural makers. The majority of iPS-dNSCs(+DLL4) differentiated to neural cells (58.66%±4.81%, GFAP; 10.90%±3.01%, Olig2; 5.00%±2.16%, PDFGra; 8.11%±4.94%, βIII; 12.66%±6.02% Nestin), while 13% remained undefined by these markers. The iPS-dNSCs that were not exposed to DLL4 did have a subset which differentiated to neural cells (9.03%±2.12% GFAP;

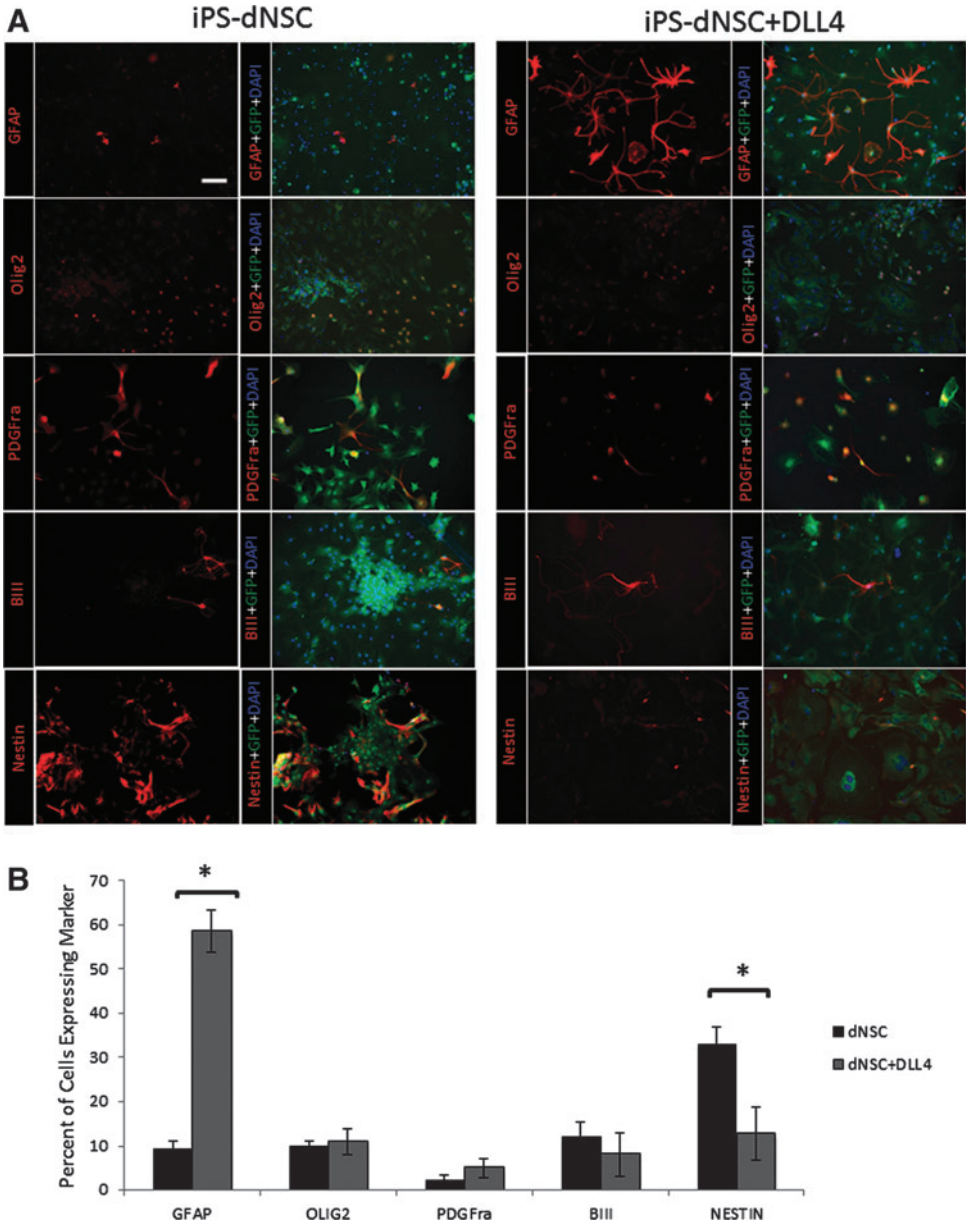

FIG. 5. In vitro differentiation pattern of iPS-dNSCs(+DLL4) 1 week following plating with 1% fetal bovine serum shows greater neural differentiation compared to iPS-dNSCs(−DLL4). **(A)** Immunofluorescence images of neural markers (GFAP; astrocytes. Olig2; oligodendrocytes and precursors. PDGFrα; immature oligodendrocytes. βIII-tublin; neurons. Nestin; NSCs). **(B)** Cell counting for immunofluorescent-positive cell shows the differentiation pattern for iPS-dNSCs cultured±DLL4. iPS-dNSC(+DLL4) yielded predominantly terminally differentiated neural cells, specifically astrocytes, while the majority of iPS-dNSC differentiated cells remained Nestin-positive or were undefined (C5-4A iPSC line) mean±SEM; $^*P<0.05$ scale bar represents 50 μm.

9.74%±1.22% Olig2; 1.93%±1.39% PDFGra; 11.90%±3.51% βIII; 32.84%±4.11% Nestin); however, the majority of cells were undefined by the neural markers, with Nestin+ cells as the next most abundant type. There were significantly more GFAP+ cells ($P=0.001$) and significantly fewer Nestin+ cells ($P=0.023$) from iPS-dNSCs(+DLL4) (Fig. 5B). These results suggest that NOTCH agonism improved the generation of iPS-dNSCs, which is reflected in their ability to form terminally differentiated neural cells.

DLL4-treated iPS-dNSCs differentiate into functional neural cells

While immunocytochemistry can be used to determine protein expression, it cannot determine whether these channels are functional. Thus, using electrophysiology in conjunction with immunocytochemistry and molecular biology, we compared whether the cells generated behave in a manner similar to endogenous neural cells. The membrane properties of the differentiated iPS-dNSCs(+DLL4) were studied using the perforated configuration of whole cell patch-clamp electrophysiology. Initial selection of various cell types was based on cell-specific morphology under phase-contrast microscopy. After recordings, the cell membrane was ruptured and intracellular milieu was backfilled with Lucifer yellow for cell identification using immunocytochemistry. A total of 39 cells were recorded. These included both neuronal and glial cells at various stages of differentiation.

Neurons were identified by their large soma and various neurite outgrowths. After the initial patch was generated, these cells had a resting membrane potential of 55.3±4.4 mV and capacitance of 26.3±4.2 pF. Input resistance was calculated by generating 30 mV pulses from −70 mV and was determined to be 128.6±55.2 MΩ. Initial voltage-clamp recordings indicated an inward current that initiated at −35.2±5.9 mV and terminated at −15.6±4.7 mV (Fig. 6A). During current-clamp recording conditions, these cells spontaneously generated fast action potentials that were sensitive to the voltage-gated Na^+ channel blocker tetrodotoxin (0.5 μM; Fig. 6B). The frequency of spontaneous action potentials was 1.3±0.8 Hz. After recording, the identity of these cells was confirmed using immunocytochemistry, probing for the neuron-specific marker βIII-tubulin (Fig. 6C).

In contrast to the spontaneously active neurons, glial cells exhibited a uniquely different electrophysiological profile. The membrane resting potentials of oligodendroglial precursor cells (OPCs) and mature oligodendrocytes were −58.6±7.1 mV and −55.4±5.9 mV, respectively; there was no significant difference between the cell types. In astrocytes, the resting membrane potential was −56.7±4.4 mV. Cell capacitance was not significantly different between the cell types (Fig. 6G). Cells that were later established to be OPCs generally had a higher input resistance of 924±69.8 MΩ, while mature oligodendrocytes were significantly lower, at 130.9±72.3 MΩ. Astrocytes were also observed to have generally low input resistance 45.1±8.6 MΩ. Outward currents in both OPCs and mature oligodendrocytes were observed to be voltage-dependent (Fig. 6D, E) with a higher inward-rectifying component in OPCs. In contrast, astrocytes did not exhibit any voltage-dependent currents (Fig. 6G). No spontaneous activity was observed in any of the glial cell types studied. After electrophysiological recordings, the cell type was confirmed using immunocytochemistry.

Discussion

Variability in neuralization propensity among NSCs from pluripotent sources

The effectiveness of the default pathway to generate dNSCs from ESCs has been characterized by our laboratory and others [16,17,28]. However, we have shown that when using the default pathway of neuralization to generate clonally derived, LIF-dependent colonies of pNSCs followed by LIF-independent dNSCs from iPSCs to neural restricted stem cells, variable results are obtained compared to ES-dNSCs. Differences in the neural propensity of murine and human pluripotent cells have previously been shown from NSCs that used embryoid body (EB) formation [31–33]. Differentiation protocols to generate NSCs from pluripotent cells that use EB formation contain an inherent risk of non-neural cells persisting in later passages. For example, oligodendrocyte progenitors derived from ESCs in media containing retinoic acid, noggin, FGF2, and platelet derived growth factor can lead to teratoma formation, likely a result of nonspecific differentiation associated with EB formation [34]. To address this potential source of nonspecific differentiation, we generated NSCs directly from pluripotent cells using the default pathway, circumventing EB formation [16,17,28]. Furthermore, we passaged single primary primitive neurospheres to secondary primitive neurospheres as well as for all passages using a low cell density (10 cell/μL). Last, all ESC and iPSC lines were cultured in parallel to avoid variation in the cell culture technique affecting the results. Even though these precautions were taken, the dNSCs generated from iPSC sources were observed to have retained pluripotent markers as well as to express nonectoderm lineages markers (Fig. 1).

There is evidence that extensive variability exists between ESC lines. The spontaneous, as well as directed, differentiation of a number of ESC lines showed significant variation in lineage propensity [35]. These differences were maintained even in late passage cell lines. It was postulated that this could be the result of genetic and epigenetic differences from an outbred population. The variable neural propensity we observed may be due to, or exacerbated by, such key differences in ESC and iPSC lines [9,36]. Given the relative ease and variability in the iPSC generation, which results in vast numbers of iPSC lines being created, effective and efficient methods, such as NOTCH agonism during neural induction, to generate restricted NSCs regardless of intrinsic differences is clearly required.

The most comprehensive evaluation of neuralization and safety of NSCs from iPSC sources examined 36 mouse iPSC lines generated using 11 different iPSC methodologies [32]. Teratoma formation assays were performed in immune-deficient mice that received transplantation of secondary NSCs, generated through EB formation, into the brain. These researchers observed a number of iPSC lines that were highly tumorigenic, even in instances, where c-myc was not transduced and no reprogramming transgene reactivation was observed. The safety of cell lines is correlated to retention of the pluripotency marker, *Nanog* [32]. Given this correlation

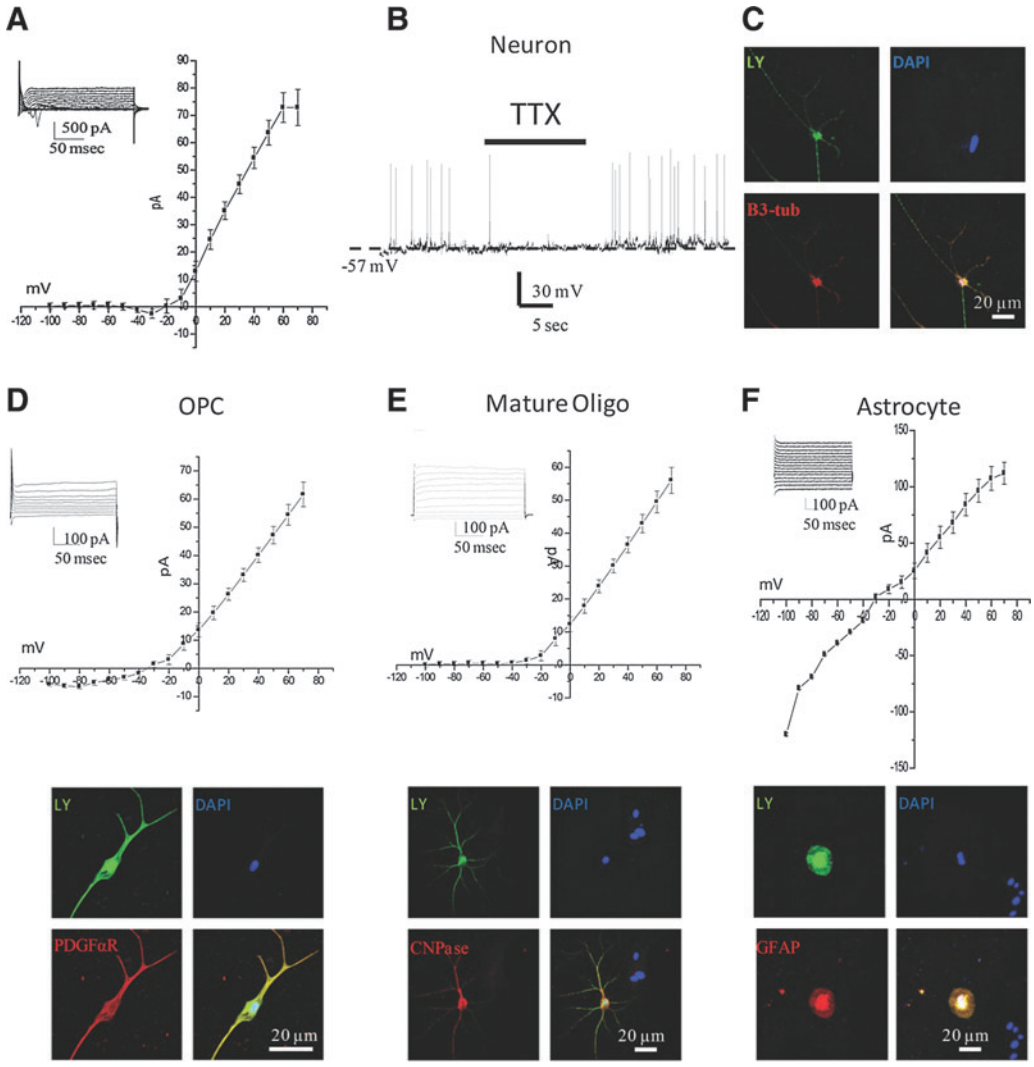

G

	Neuron	OPC	Mature Oligo	Astrocytes
Em (mV) (@rest)	-55.3 ± 4.4	-58.6 ± 7.1	-55.4 ± 5.9	-56.7 ± 4.4
Input (MΩ)	128.6 ± 55.2	924.1 ± 69.8	130.9 ± 72.3	45.1 ± 8.6
Capacitance (pF)	26.3 ± 4.2	16.7 ± 3.3	20.1 ± 4.1	17.4 ± 4.8
N=	12	7	10	10

FIG. 6. Electrophysiological profile of differentiated cells derived from iPSCs. Using the nystatin configuration of the patch-clamp electrophysiology method, both inward and outward currents were recorded in differentiated cells. In some cells, a distinct inward current starting at −30 mV and terminating around −10 mV **(A)** was observed. Inset depicts a typical current profile of voltage steps from −100 mV to +80 mV. During current-clamp studies, neuronal-like cells were observed to have reversible depolarizing transients that were sensitive to bath application of the voltage sensitive Na+ channel blocker tetrodotoxin (TTX 0.5 mM) **(B)**. After electrophysiological experiments, the cells were backfilled with Lucifer yellow [**(C)** *green*) and cells were found to be immunopositive for the neuronal marker β-3 tubulin (*red*). In contrast, glial cells did not exhibit any inward current profile, although they did show current/voltage relationships typical for oligodendroglial precursor cells [OPC; **(D)**], mature oligodendrocytes **(E)**, and astrocytes **(F)**. After electrophysiological recordings, cells were backfilled with Lucifer yellow (LY; *green*). Cells were identified as being OPCs when stained positive for PDGFα-R [**(D)**; *red*), as mature oligodendrocytes when positive for myelin basic protein [**(E)**; MBP; *red*], or astrocytes when positive for GFAP [**(E)**; *red*]. Table **(G)** summarizes the electrophysiological profile of the above cells indicating resting membrane potential (Em in mV), input resistance (MΩ), membrane capacitance (pF), and number of cells recorded (N).

between retention of pluripotency marker and teratoma formation, our data showing that iPS-dNSCs(+DLL4) have a greater decrease in pluripotency gene markers compared to the iPS-dNSCs(−DLL4) (Fig. 4) suggest that NOTCH agonism could increase the safety and clinical translation potential of these cells for in vivo use. However, in terms of clinical translation, screening for safety is of the utmost importance and will require in vivo validation of these cells.

Extensive screening for safety of multiple iPSC lines is time-consuming and may not always be possible in situations, where only limited cells lines are generated. Furthermore, the iPSCs used in this study have been validated using chimera formation and tetrapoid embryo complementation [11], but variation in the dNSCs produced persists, indicating that screening will be required for every differentiated product of the iPSC line rather than simply at the pluripotent level. This reiterates the value of creating culture conditions that can consistently and reliably produce dNSCs from different iPSC lines.

The effect of Noggin on primary neurosphere generation

Initially, we hypothesized that neuralization could be improved by the addition of Noggin. Noggin binds extracellularly to the neural inhibitor BMP, specifically BMP4 [37]. Noggin has been shown to reinforce the neuralization of murine ESCs by increasing the number of neurospheres generated [16,17]. However, its effect on the character or quality of neurospheres has not been determined. When Noggin was added to SFM with LIF, there was a significant increase in neurospheres generated (Fig. 2B). Also, since Noggin did not affect neurosphere generation when added to ESC/iPSC expansion, we can conclude that there is no preselection of neural precursors before default conditions. There was no change in the mRNA profile with a variety of durations of Noggin treatment, indicating that iPSCs effectively generate pNSCs with a standard serum-free condition and that Noggin treatment only increases the cell number. Also, the lack of effect of Noggin treatment on the subsequent dNSCs corresponds with the reports that have shown that NSCs isolated from the SVZ do not respond to BMP antagonists [38]. In contrast, this study has shown that Noggin does influence the expansion of neural precursor cells from the hippocampus. However, the neural precursor cells isolated from the hippocampus are distinct from the NSCs isolated from the SVZ or generated via the default pathways, since the hippocampal cells cannot self-renew or form neurospheres [39]. These data, combined the passage of single primary primitive neurospheres to secondary primitive neurospheres, suggest that the ineffective neuralization of the iPSCs is not due to retention of pluripotent cells from expansion conditions, but is likely to be due to poor transition from pNSCs to dNSCs.

The effect of NOTCH pathway agonism on dNSC generation

NOTCH signaling is a key regulator of neural development and has been shown to be involved in the self-renewal and proliferation of NSCs. The NOTCH pathway components are expressed throughout the brain, including the NSC niche of the SVZ. We selected to activate this critical pathway using a recombinant DLL4 protein, since the DLL family is the primary NOTCH ligand that interacts with NSCs [27] and DLL4 is the most avid of all NOTCH ligands, including both DLLs and Jaggeds [40]. Although in physiological conditions DLL4 would be membrane-bound, when interacting with the NOTCH receptor on the NSCs, the recombinant protein has been shown to agonize the receptor and induce cleavage of the NICD by γ-secratese and to propagate the signal [25]. We demonstrated that recombinant mouse DLL4 promotes the maintained expression of *Hes3* in NSCs (Fig. 3) in agreement with studies that show NOTCH receptor activation induced HES3 [25]. HES3 is highly expressed in the SVZ stem niche, upstream of the sonic hedgehog pathway, and is required for the survival of NSCs in vivo [25]. In contrast, we showed Hes1 to be unresponsive to DLL4 treatment (Supplementary Fig. S2). HES1 expression has been shown to persist even with NOTCH pathway interruption [24]. The may be due to the role of Hes1 in the early neuroepidermal stage before NOTCH and Delta expression [41]. Hes5 is also a key effector of the NOTCH pathway in NSC maturation; however, we did not examine it in this study. The importance of HES3 is further emphasized when *Hes1:Hes5* double and *Hes1:Hes3:Hes5* triple knockouts are compared. In *Hes1:Hes3:Hes5* triple knockout, neuroepithelial cells prematurely differentiated to neurons as early as E8.5, while *Hes1:Hes5* neuroepithelial cells and radial glia are maintained suggesting the compensatory role of HES3 in NSCs [42]. Many of the studies examining the role of NOTCH in neurogenesis use transgenes to express NICD or knockouts to ablate NOTCH signaling. The use of a recombinant protein, DLL4, to induce the NOTCH pathway allows us to retain a virus and mutagenesis-free system when generating dNSCs, thus not limiting their clinical application.

In addition to the NOTCH pathway, SHH and Wnt signaling are known to influence the development of NSCs and their maintenance by independent and interrelated mechanisms. SHH and Wnt signaling plays a critical role during embryonic development and modulation of these pathways affect NSC growth and regulation. These pathways have diverse functions and play key roles throughout neurogenesis. There is considerable overlap and cross talk between these pathways and NOTCH signaling. SHH expression can be upregulated in a time-dependent manner by the addition of NOTCH ligand Jagged1 in cultured NSCs [25]. WNT inhibition during neuralization acts similarly to Noggin in that the inhibition results in greater neural differentiation [43,44]. Also, WNT signaling is maintained throughout neurogenesis and could be involved in the primitive to dNSC states via modulation of FGF- dependent pathways [45]. The mechanism by which WNT modulates the NSC population may be through effects on HES gene expression [46]. We focused on the NOTCH pathway because of its specific role in the transition from pNSC to dNSC. Primitive neurospheres (LIF-dependent) from both ESCs and primary culture and from E7.5 embryos generated from NOTCH-deficient sources propagated in similar quantities to wild-type controls.[19,24] Also, the insertion of a retrovirus with active *Notch1* to ESCs did not affect LIF-dependent expansion of ESC-derived neurospheres [19]. However, in maintenance of the LIF-independent NSC population, from ESC, tertiary passage E7.5 NSC or primary culture of E8.0 NSCs, NOTCH signaling was shown to be essential [19,24]. Increased differentiation of

the NSCs was observed compared to NSCs that received active NOTCH1 retrovirus [24]. These studies suggest a mechanism of action, whereby NOTCH signaling promotes the transition from the primitive to the definitive state, while inhibiting the differentiation of the dNSCs, thereby creating an homogeneous cell population. These data support our finding that the loss of effective NOTCH signaling results in inefficient generation of dNSCs from iPSC sources and that exogenous NOTCH agonism improves the definitive state of the NSCs.

The differentiation potential of NOTCH-agonized dNSCs

The in vitro differentiation profile of the iPS-dNSCs with NOTCH agonism yielded primarily nestin-positive or undefined cells, while iPS-dNSCs grown in the presence of DLL4 differentiated mostly to glial cells, overwhelmingly astrocytes (Fig. 6). These cells displayed electrophysiological signatures similar to the respective endogenous cells [47]. The observed differentiation profile of the iPS-dNSCs(+DLL4) closely resembled the pattern observed previously and published by our laboratory for both ES-dNSCs as well as adult tissue-derived NSCs [28,48]. Furthermore, the iPS-dNSC(−DLL4) differentiation profile is more reflective of ES-pNSCs [28], reinforcing our hypothesis that induction of the NOTCH pathway enhances the generation and maintenance of dNSCs from a primitive population.

The tendency of the iPS-dNSCs(+DLL4) to differentiate mostly into astrocytes may appear problematic considering neurons or oligodendrocytes are often the desired cell fates for proposed therapies. Also, astrocytic differentiation may be detrimental in vivo following central nervous system (CNS) insult, since their contribution to the glial scar can be associated with negative outcomes such the inhibition of endogenous regeneration [49] and increased neuropathic pain [50]. Although the differentiation of these cells yielded mostly astrocytes in vitro, this may not accurately reflect the cell fate in vivo. The instructive niche of the dysmyelinated CNS of *Shiverer* mice promotes adult tissue-derived NSCs and ES-dNSCs to yield primarily myelinating oligodendrocytes even though their in vitro profile suggested astrocytic differentiation [28,48,51]. For example, through factors, such as GRO-1 or neuregulin, NG2-positive oligodendrocytes may be creating an environment that preferentially direct dNSCs to an oligodendrocytic lineage [52,53]. However, induction of the NOTCH pathway has been implicated in promoting an astrocytic differentiation [54]. This reiterates the requirement to examine the fate of the iPS-dNSCs(+DLL4) in vivo.

Conclusions

For the promise of iPSCs to be realized in the field of regenerative medicine, methods to consistently and effectively generate neural cells from any iPSC line regardless of intrinsic differences in neural propensity are required. Using the recombinant protein DLL4 to induce the NOTCH signaling pathway, we were able to improve the neuralization of PB transposon reprogrammed cells.

Acknowledgments

This project was funded by the Canadian Institutes of Health Research (CIHR; grant reference: NHG 99090), Wings for Life Spinal Research Trust and the McEwen Center for Regenerative Medicine. R.P.S. received funding from Ontario Neurotrauma Foundation and CIHR Training Programs in Regenerative Medicine. M.G.F. is the Gerald and Tootsie Halbert Chair in Neural Repair and Regeneration.

Author Disclosure Statement

No competing financial interests exist.

References

1. Goldman S. (2005). Stem and progenitor cell-based therapy of the human central nervous system. Nat Biotechnol 23: 862–871.
2. Eftekharpour E, S Karimi-Abdolrezaee and MG Fehlings. (2008). Current status of experimental cell replacement approaches to spinal cord injury. Neurosurg Focus 24:E19.
3. Karimi-Abdolrezaee S, E Eftekharpour, J Wang, CM Morshead and MG Fehlings. (2006). Delayed transplantation of adult neural precursor cells promotes remyelination and functional neurological recovery after spinal cord injury. J Neurosci 26:3377–3389.
4. Keirstead HS, G Nistor, G Bernal, M Totoiu, F Cloutier, K Sharp and O Steward. (2005). Human embryonic stem cell-derived oligodendrocyte progenitor cell transplants remyelinate and restore locomotion after spinal cord injury. J Neurosci 25:4694–4705.
5. Takagi Y, J Takahashi, H Saiki, A Morizane, T Hayashi, Y Kishi, H Fukuda, Y Okamoto, M Koyanagi, et al. (2005). Dopaminergic neurons generated from monkey embryonic stem cells function in a Parkinson primate model. J Clin Invest 115:102–109.
6. Pluchino S, A Quattrini, E Brambilla, A Gritti, G Salani, G Dina, R Galli, U Del Carro, S Amadio, et al. (2003). Injection of adult neurospheres induces recovery in a chronic model of multiple sclerosis. Nature 422:688–694.
7. Corti S, M Nizzardo, M Nardini, C Donadoni, S Salani, D Ronchi, F Saladino, A Bordoni, F Fortunato, et al. (2008). Neural stem cell transplantation can ameliorate the phenotype of a mouse model of spinal muscular atrophy. J Clin Invest 118:3316–3330.
8. Takahashi K, K Tanabe, M Ohnuki, M Narita, T Ichisaka, K Tomoda and S Yamanaka. (2007). Induction of pluripotent stem cells from adult human fibroblasts by defined factors. Cell 131:861–872.
9. Takahashi K and S Yamanaka. (2006). Induction of pluripotent stem cells from mouse embryonic and adult fibroblast cultures by defined factors. Cell 126:663–676.
10. Zhao T, ZN Zhang, Z Rong and Y Xu. (2011). Immunogenicity of induced pluripotent stem cells. Nature 474: 212–215.
11. Woltjen K, IP Michael, P Mohseni, R Desai, M Mileikovsky, R Hamalainen, R Cowling, W Wang, P Liu, et al. (2009). piggyBac transposition reprograms fibroblasts to induced pluripotent stem cells. Nature 458:766–770.
12. Zhou H, S Wu, JY Joo, S Zhu, DW Han, T Lin, S Trauger, G Bien, S Yao, et al. (2009). Generation of induced pluripotent stem cells using recombinant proteins. Cell Stem Cell 4: 381–384.
13. Yu J, K Hu, K Smuga-Otto, S Tian, R Stewart, Slukvin, II and JA Thomson. (2009). Human induced pluripotent stem cells free of vector and transgene sequences. Science 324:797–801.
14. Kaji K, K Norrby, A Paca, M Mileikovsky, P Mohseni and K Woltjen. (2009). Virus-free induction of pluripotency and

subsequent excision of reprogramming factors. Nature 458:771–775.
15. Bilic J and JC Izpisua Belmonte. (2011). Concise review: induced pluripotent stem cells versus embryonic stem cells: close enough or yet too far apart? Stem Cells 30:33–41.
16. Smukler SR, SB Runciman, S Xu and D van der Kooy. (2006). Embryonic stem cells assume a primitive neural stem cell fate in the absence of extrinsic influences. J Cell Biol 172:79–90.
17. Tropepe V, S Hitoshi, C Sirard, TW Mak, J Rossant and D van der Kooy. (2001). Direct neural fate specification from embryonic stem cells: a primitive mammalian neural stem cell stage acquired through a default mechanism. Neuron 30:65–78.
18. Tropepe V, M Sibilia, BG Ciruna, J Rossant, EF Wagner and D van der Kooy. (1999). Distinct neural stem cells proliferate in response to EGF and FGF in the developing mouse telencephalon. Dev Biol 208:166–188.
19. Hitoshi S, RM Seaberg, C Koscik, T Alexson, S Kusunoki, I Kanazawa, S Tsuji and D van der Kooy. (2004). Primitive neural stem cells from the mammalian epiblast differentiate to definitive neural stem cells under the control of Notch signaling. Genes Dev 18:1806–1811.
20. Wood HB and V Episkopou. (1999). Comparative expression of the mouse Sox1, Sox2 and Sox3 genes from pre-gastrulation to early somite stages. Mech Dev 86:197–201.
21. Yoon K and N Gaiano. (2005). Notch signaling in the mammalian central nervous system: insights from mouse mutants. Nat Neurosci 8:709–715.
22. Louvi A and S Artavanis-Tsakonas. (2006). Notch signalling in vertebrate neural development. Nat Rev Neurosci 7:93–102.
23. Nakamura Y, S Sakakibara, T Miyata, M Ogawa, T Shimazaki, S Weiss, R Kageyama and H Okano. (2000). The bHLH gene hes1 as a repressor of the neuronal commitment of CNS stem cells. J Neurosci 20:283–293.
24. Hitoshi S, T Alexson, V Tropepe, D Donoviel, AJ Elia, JS Nye, RA Conlon, TW Mak, A Bernstein and D van der Kooy. (2002). Notch pathway molecules are essential for the maintenance, but not the generation, of mammalian neural stem cells. Genes Dev 16:846–858.
25. Androutsellis-Theotokis A, RR Leker, F Soldner, DJ Hoeppner, R Ravin, SW Poser, MA Rueger, SK Bae, R Kittappa and RD McKay. (2006). Notch signalling regulates stem cell numbers *in vitro* and *in vivo*. Nature 442:823–826.
26. Stump G, A Durrer, AL Klein, S Lutolf, U Suter and V Taylor. (2002). Notch1 and its ligands Delta-like and Jagged are expressed and active in distinct cell populations in the postnatal mouse brain. Mech Dev 114:153–159.
27. Ables JL, JJ Breunig, AJ Eisch and P Rakic. (2011). Not(ch) just development: Notch signalling in the adult brain. Nat Rev Neurosci 12:269–283.
28. Rowland JW, JJ Lee, RP Salewski, E Eftekharpour, D van der Kooy and MG Fehlings. (2011). Generation of neural stem cells from embryonic stem cells using the default mechanism: *in vitro* and *in vivo* characterization. Stem Cells Dev 20:1829–1845.
29. Reynolds BA and S Weiss. (1996). Clonal and population analyses demonstrate that an EGF-responsive mammalian embryonic CNS precursor is a stem cell. Dev Biol 175:1–13.
30. Schmittgen TD and KJ Livak. (2008). Analyzing real-time PCR data by the comparative C(T) method. Nat Protoc 3:1101–1108.
31. Kim DS, JS Lee, JW Leem, YJ Huh, JY Kim, HS Kim, IH Park, GQ Daley, DY Hwang and DW Kim. (2010). Robust enhancement of neural differentiation from human ES and iPS cells regardless of their innate difference in differentiation propensity. Stem Cell Rev 6:270–281.
32. Miura K, Y Okada, T Aoi, A Okada, K Takahashi, K Okita, M Nakagawa, M Koyanagi, K Tanabe, et al. (2009). Variation in the safety of induced pluripotent stem cell lines. Nat Biotechnol 27:743–745.
33. Wang A, Z Tang, IH Park, Y Zhu, S Patel, GQ Daley and S Li. (2011). Induced pluripotent stem cells for neural tissue engineering. Biomaterials 32:5023–5032.
34. Sadowski D, ME Kiel, M Apicella, AG Arriola, CP Chen and RD McKinnon. (2010). Teratogenic potential in cultures optimized for oligodendrocyte development from mouse embryonic stem cells. Stem Cells Dev 19:1343–1353.
35. Osafune K, L Caron, M Borowiak, RJ Martinez, CS Fitz-Gerald, Y Sato, CA Cowan, KR Chien and DA Melton. (2008). Marked differences in differentiation propensity among human embryonic stem cell lines. Nat Biotechnol 26:313–315.
36. Kim K, A Doi, B Wen, K Ng, R Zhao, P Cahan, J Kim, MJ Aryee, H Ji, et al. (2010). Epigenetic memory in induced pluripotent stem cells. Nature 467:285–290.
37. Hemmati-Brivanlou A and DA Melton. (1994). Inhibition of activin receptor signaling promotes neuralization in *Xenopus*. Cell 77:273–281.
38. Bonaguidi MA, CY Peng, T McGuire, G Falciglia, KT Gobeske, C Czeisler and JA Kessler. (2008). Noggin expands neural stem cells in the adult hippocampus. J Neurosci 28:9194–9204.
39. Seaberg RM and D van der Kooy. (2002). Adult rodent neurogenic regions: the ventricular subependyma contains neural stem cells, but the dentate gyrus contains restricted progenitors. J Neurosci 22:1784–1793.
40. D'Souza B, L Meloty-Kapella and G Weinmaster. (2010). Canonical and non-canonical Notch ligands. Curr Top Dev Biol 92:73–129.
41. Kageyama R, T Ohtsuka, J Hatakeyama and R Ohsawa. (2005). Roles of bHLH genes in neural stem cell differentiation. Exp Cell Res 306:343–348.
42. Hatakeyama J, Y Bessho, K Katoh, S Ookawara, M Fujioka, F Guillemot and R Kageyama. (2004). Hes genes regulate size, shape and histogenesis of the nervous system by control of the timing of neural stem cell differentiation. Development 131:5539–5550.
43. Aubert J, H Dunstan, I Chambers and A Smith. (2002). Functional gene screening in embryonic stem cells implicates Wnt antagonism in neural differentiation. Nat Biotechnol 20:1240–1245.
44. Watanabe K, D Kamiya, A Nishiyama, T Katayama, S Nozaki, H Kawasaki, Y Watanabe, K Mizuseki and Y Sasai. (2005). Directed differentiation of telencephalic precursors from embryonic stem cells. Nat Neurosci 8:288–296.
45. Dang LT and V Tropepe. (2010). FGF dependent regulation of Zfhx1b gene expression promotes the formation of definitive neural stem cells in the mouse anterior neurectoderm. Neural Dev 5:13.
46. Hirsch C, LM Campano, S Wohrle and A Hecht. (2007). Canonical Wnt signaling transiently stimulates proliferation and enhances neurogenesis in neonatal neural progenitor cultures. Exp Cell Res 313:572–587.
47. Buttigieg J, E Eftekharpour, S Karimi-Abdolrezaee and MG Fehlings. (2011). Molecular and electrophysiological evidence for the expression of BK channels in oligodendroglial precursor cells. Eur J Neurosci 34:538–547.
48. Eftekharpour E, S Karimi-Abdolrezaee, J Wang, H El Beheiry, C Morshead and MG Fehlings. (2007). Myelination of

congenitally dysmyelinated spinal cord axons by adult neural precursor cells results in formation of nodes of Ranvier and improved axonal conduction. J Neurosci 27:3416–3428.
49. Wilhelmsson U, L Li, M Pekna, CH Berthold, S Blom, C Eliasson, O Renner, E Bushong, M Ellisman, TE Morgan and M Pekny. (2004). Absence of glial fibrillary acidic protein and vimentin prevents hypertrophy of astrocytic processes and improves post-traumatic regeneration. J Neurosci 24:5016–5021.
50. Gwak YS, J Kang, GC Unabia and CE Hulsebosch. (2012). Spatial and temporal activation of spinal glial cells: role of gliopathy in central neuropathic pain following spinal cord injury in rats. Exp Neurol 234:362–372.
51. Windrem MS, MC Nunes, WK Rashbaum, TH Schwartz, RA Goodman, G McKhann, 2nd, NS Roy and SA Goldman. (2004). Fetal and adult human oligodendrocyte progenitor cell isolates myelinate the congenitally dysmyelinated brain. Nat Med 10:93–97.
52. Canoll PD, JM Musacchio, R Hardy, R Reynolds, MA Marchionni and JL Salzer. (1996). GGF/neuregulin is a neuronal signal that promotes the proliferation and survival and inhibits the differentiation of oligodendrocyte progenitors. Neuron 17:229–243.
53. Wu Q, RH Miller, RM Ransohoff, S Robinson, J Bu and A Nishiyama. (2000). Elevated levels of the chemokine GRO-1 correlate with elevated oligodendrocyte progenitor proliferation in the jimpy mutant. J Neurosci 20:2609–2617.
54. Namihira M, J Kohyama, K Semi, T Sanosaka, B Deneen, T Taga and K Nakashima. (2009). Committed neuronal precursors confer astrocytic potential on residual neural precursor cells. Dev Cell 16:245–255.

Address correspondence to:
Dr. Michael G. Fehlings
Institute of Medical Science
University of Toronto
399 Bathurst Street
Toronto, Ontario M5T 2S8
Canada

E-mail: michael.fehlings@uhn.on.ca

Received for publication April 24, 2012
Accepted after revision August 13, 2012
Prepublished on Liebert Instant Online August 13, 2012